I Research: Journal of Pharmacology
www.iresearchonline.com

Evaluation of the Cardioprotective Activity of Rutin Phytosome Against Doxorubicin-Induced Cardiotoxicity by using Animal model

Karthikeyan M * and Jegan N.

Department of Pharmacology, K.M College of Pharmacy, The Tamil Nadu Dr. M.G.R Medical University, Chennai, Tamil Nadu, India

ARTICLE INFO

Keywords:
Rutin phytosome,
Doxorubicin,
Cardiotoxicit,
Phosphatidylcholine,
Antioxidant,
Cardioprotection,
Wistar rats.

Article History:
Received : 23rd September 2026
Accepted : 26th September 2026
Available online : 26th September 2026

ABSTRACT

Background: Doxorubicin remains a cornerstone anticancer agent, but its clinical utility is limited by dose-dependent cardiotoxicity mediated largely through oxidative stress and mitochondrial injury. Rutin, a flavonoid glycoside with well-documented antioxidant activity, is constrained therapeutically by poor aqueous solubility and limited membrane permeability. Complexation with phosphatidylcholine to form a phytosome was investigated as a strategy to overcome these limitations and enhance cardioprotective efficacy.

Methods: Rutin phytosome was prepared by the thin-film hydration/solvent-evaporation technique at three rutin-to-phosphatidylcholine ratios (1:0.5, 1:1, 1:1.5) and characterised by entrapment efficiency, Fourier-transform infrared (FTIR) spectroscopy, scanning electron microscopy (SEM), and *in vitro* dialysis-membrane drug release. The optimised formulation was evaluated *in vivo* in a five-group Wistar rat model of doxorubicin-induced cardiotoxicity (normal control; toxic control, doxorubicin 20 mg/kg i.p.; standard, carvedilol 30 mg/kg; test drug, rutin 50 mg/kg; test formulation, rutin phytosome 50 mg/kg), with cardiac biomarkers (CK-MB, LDH, troponin-I), myocardial antioxidant parameters (SOD, CAT, MDA), and histopathology as endpoints.

Results: The 1:1 formulation (F2) gave the highest entrapment efficiency (94.2%). FTIR confirmed retention of rutin's characteristic bands with shifts indicative of hydrogen bonding, and SEM showed irregular, rough-surfaced, predominantly spherical particles. *In vitro* release was sustained, reaching 83.1% cumulative release at 6 hours. *In vivo*, doxorubicin produced marked elevation of CK-MB, LDH and troponin-I and depletion of SOD and CAT with elevated MDA, confirming cardiotoxicity. Pretreatment with rutin phytosome produced a greater reduction in all three cardiac biomarkers than plain rutin (CK-MB 34.14 ± 0.49 vs 38.68 ± 0.62 U/L; LDH 253.2 ± 3.83 vs 291.4 ± 3.97 IU/L; troponin-I 0.79 ± 0.037 vs 2.08 ± 0.020 ng/mL) and better restoration of antioxidant status, findings corroborated by graded histopathological recovery of myocardial architecture.

Introduction

Breast cancer is the most commonly diagnosed cancer among women and one of the leading causes of cancer mortality globally. According to GLOBOCAN 2022 estimates compiled by the International Agency for Research on Cancer, breast cancer accounted for

Cardiovascular disease and cancer are together the two leading causes of death worldwide, and their intersection cardiotoxicity arising from anticancer chemotherapy has become a major clinical concern over the past three decades. Global cancer statistics for 2022 recorded approximately 20 million new cases and 9.7 million deaths, with roughly one in nine men and one in twelve women expected to die of cancer during their lifetime [1,2]. The growing population of long-term cancer survivors remains vulnerable to delayed cardiac toxicity from the very therapies that extended survival.

Among chemotherapeutic classes, anthracyclines are valued for broad efficacy against haematological and solid tumours, but this benefit is offset by dose-limiting cardiotoxicity. Doxorubicin, the prototypical anthracycline, remains central to regimens for breast cancer, lymphoma, leukaemia and sarcoma more than five decades after its introduction, which sustains research interest in agents that can protect the myocardium without compromising antitumour activity [3,4]. In resource-limited settings such as India, doxorubicin's comparatively low cost keeps it in wide use even where advanced cardiac-surveillance infrastructure is unevenly

* Corresponding author
✉: Karthikeyan M: karthikeyan232000@gmail.com

available, making an inexpensive, orally administrable adjuvant cardioprotectant particularly valuable [3,4].

Doxorubicin exerts antitumour activity through DNA intercalation, topoisomerase-II inhibition and generation of reactive oxygen species (ROS) via redox cycling of its quinone moiety [5,6]. The same redox chemistry underlies its cardiotoxicity: cardiomyocytes are particularly vulnerable because of their high mitochondrial density, limited antioxidant reserve and largely non-regenerative nature. Doxorubicin accumulates in cardiac mitochondria owing to its affinity for cardiolipin, amplifying local ROS generation, impairing electron transport and ATP synthesis, and disrupting iron homeostasis to further catalyse hydroxyl-radical formation [5,7]. Cardiomyocytes also express topoisomerase IIβ, and formation of a Top2β–doxorubicin–DNA cleavage complex produces double-strand DNA breaks that suppress mitochondrial-biogenesis signalling (PGC-1α/β) and activate p53-mediated cell death, linking the drug's antitumour mechanism directly to cardiac injury [6,7]. Oxidative modification of calcium-handling proteins (RyR2, SERCA2a) causes calcium overload and contractile dysfunction, while chronic activation of apoptotic and inflammatory pathways (NF-κB, TNF-α, IL-6) drives progressive myocardial fibrosis [3,8,9]. The clinical course may present acutely as transient arrhythmia, or as early- or late-onset chronic cardiomyopathy, with cumulative dose above 400–550 mg/m^2 sharply increasing the risk of heart failure [9].

Existing cardioprotective strategies, principally the iron-chelating agent dexrazoxane, carry limitations in efficacy, cost and potential interference with antitumour activity, which has driven interest in naturally derived antioxidants as adjuvant agents [10–14]. Flavonoids, in particular, have attracted attention for their free-radical-scavenging and membrane-stabilising properties in the context of anthracycline cardiotoxicity [15].

Rutin (quercetin-3-O-rutinoside) is a dietary flavonoid glycoside with well-documented antioxidant, anti-inflammatory and free-radical-scavenging activity [16,17]. Prior work has reported cardioprotective effects of rutin in chemically induced injury models, including attenuation of inflammatory markers in diabetic rats [18] and protection against doxorubicin-and pirarubicin-induced cardiac and renal toxicity through modulation of autophagy and apoptosis [58,68,69]. However, its poor aqueous solubility and limited intestinal membrane permeability constrain systemic bioavailability and, consequently, its therapeutic utility [16,17].

Phytosome technology, in which a plant-derived polyphenol is complexed with a phospholipid such as phosphatidylcholine, has emerged as an approach to overcome these bioavailability limitations. The phospholipid's hydrophilic phosphate head anchors to polar hydroxyl groups of the phenolic substrate while the lipophilic fatty-acid tails remain free, conferring the resulting complex with both hydrophilic and lipophilic character that facilitates passage across the lipid-rich intestinal epithelium [19,20]. Rutin–phospholipid complexes have previously been reported to improve entrapment, stability and dissolution behaviour relative to free rutin [19,47,52,59,61,66,67], but their cardioprotective potential against doxorubicin-induced cardiotoxicity has not been extensively characterised.

The present study was therefore designed with two objectives: (i) to formulate and characterise a rutin phytosome complex, optimising the rutin-to-phosphatidylcholine ratio for maximal.

entrapment efficiency and confirming complexation by FTIR and SEM together with *in vitro* release behaviour; and (ii) to evaluate the cardioprotective activity of the optimised rutin phytosome, relative to free rutin and the standard cardioprotectant carvedilol, in a doxorubicin-induced cardiotoxicity model in Wistar rats, using cardiac biomarkers, myocardial antioxidant status and histopathology as endpoints.

Materials and Methods

Chemicals

Rutin was procured from Universal Scientific Appliances Pvt. Ltd., and doxorubicin from Jayam Life Sciences, K.K. Nagar, Madurai. Soya lecithin (phosphatidylcholine) and all other chemicals used were of analytical grade and were obtained from local suppliers.

Preparation of Rutin Phytosome

Rutin phytosome was prepared by a solvent-evaporation/thin-film hydration technique [53]. Rutin and phosphatidylcholine were accurately weighed in defined weight ratios and dissolved separately in a minimal volume of anhydrous ethanol. The two solutions were combined in a round-bottom flask and stirred continuously on a magnetic stirrer at 40–50 °C for approximately 6 hours to allow complex formation. The ethanol was then removed under reduced pressure using a rotary evaporator until a thin dry film formed on the flask wall. The film was scraped, dried further under vacuum to remove residual solvent, pulverised, passed through a sieve to obtain a uniform powder, and stored in an airtight, light-protected container at 2–8 °C until further evaluation.

Three formulations were prepared at rutin-to-phosphatidylcholine weight ratios of 1:0.5 (F1), 1:1 (F2) and 1:1.5 (F3) to identify the ratio giving optimal

entrapment efficiency. In the proposed mechanism of complexation, the hydrophilic phosphate head of phosphatidylcholine forms hydrogen bonds with the polar hydroxyl groups on the A and B rings of rutin, while the lipophilic fatty-acid tails remain outward-facing, conferring the resulting complex with amphiphilic character suited to crossing the lipid-rich intestinal epithelium.

Physicochemical Characterisation

Calibration curve: A stock solution of rutin (100 µg/mL) in ethanol was serially diluted to give working standards of 20–100 µg/mL. Absorbance was measured by UV–visible spectrophotometry at the determined λmax (≈257 nm in ethanol), and a linear regression of concentration against absorbance was constructed.

Entrapment efficiency (EE%): Each formulation, equivalent to 100 mg rutin, was suspended in methanol and centrifuged to separate free (unentrapped) drug in the supernatant from complexed drug. The rutin concentration in the supernatant was determined spectrophotometrically at 370 nm, and EE% was calculated as [(total drug − free drug)/total drug] × 100.

FTIR spectroscopy: Spectra of pure rutin and the optimised rutin phytosome were recorded using the KBr-pellet technique over 4000–400 cm^{-1} at 4 cm^{-1} resolution (16–32 scans averaged), to identify shifts, broadening or attenuation of characteristic rutin absorption bands (O–H stretching near 3400 cm^{-1}, aromatic C=C, C–O–C/C–O) indicative of hydrogen-bonded complexation with phosphatidylcholine.

Scanning electron microscopy (SEM): Surface morphology of the dried, gold-sputter-coated phytosome powder was examined at an accelerating voltage of 10–20 kV to assess particle shape, surface texture and aggregation.

In vitro drug release: Release was assessed by the dialysis-membrane method. Rutin phytosome (20 mg) was dispersed in distilled water, sealed within an activated dialysis membrane, and immersed in 50 mL distilled water at 25 ± 0.5 °C with stirring at ~150 rpm for 6 hours. Aliquots were withdrawn at intervals, replaced with fresh medium, and analysed spectrophotometrically at 370 nm; cumulative percentage drug release was calculated against the calibration curve.

Experimental Animals

Wistar albino rats of either sex (20–24 weeks, 150–200 g) were obtained from the animal house of K.M. College of Pharmacy, Madurai, and acclimatised for 15 days under standard conditions (23 ± 1 °C, 50 ± 10% relative humidity, 12 h/12 h light/dark cycle) with free access to standard pelleted diet and water. All procedures were conducted in accordance with CPCSEA guidelines and approved by the Institutional Animal Ethics Committee of K.M. College of Pharmacy, Madurai.

Induction of Cardiotoxicity and Treatment Protocol

Twenty-five animals (n = 5 per group) were randomly allocated to five groups. Rutin was suspended in 0.5% carboxymethylcellulose (CMC) and administered orally at 50 mg/kg; carvedilol tablets were triturated and dissolved in 0.5% CMC for oral administration at 30 mg/kg; rutin phytosome was suspended in 0.5% CMC and administered orally at 50 mg/kg; doxorubicin was dissolved in normal saline and administered intraperitoneally at 20 mg/kg. [60]

Table 1. Group allocation and treatment protocol.

Group	Treatment
I – Normal control	No doxorubicin, no test drug; maintained under normal conditions
II – Toxic control	Single intraperitoneal dose of doxorubicin 20 mg/kg on Day 14 [55,64]
III – Standard	Carvedilol 30 mg/kg orally, Days 1–13; doxorubicin 20 mg/kg i.p. on Day 14 [55]
IV – Test drug	Rutin 50 mg/kg orally, Days 1–13; doxorubicin 20 mg/kg i.p. on Day 14 [65]
V – Test formulation	Rutin phytosome 50 mg/kg orally, Days 1–13; doxorubicin 20 mg/kg i.p. on Day 14

Sample Collection

On Day 16 (48 hours after doxorubicin challenge), animals were anaesthetised and blood was withdrawn by retro-orbital plexus or cardiac puncture for serum separation and biomarker estimation. Animals were then sacrificed and the heart excised, rinsed in ice-cold normal saline, blotted and weighed. A portion of cardiac tissue was homogenised for antioxidant/lipid-peroxidation assays; the remainder was fixed in 10% neutral buffered formalin for histopathology.

Biochemical Parameters

Serum creatine kinase-MB (CK-MB), lactate dehydrogenase (LDH) and cardiac troponin-I (TnI) were estimated as indices of myocardial membrane injury; their release into circulation reflects loss of cardiomyocyte membrane integrity following doxorubicin-induced oxidative damage [55]. In heart-tissue homogenate, superoxide dismutase (SOD) and catalase (CAT) activities were estimated as markers of enzymatic antioxidant defence, and malondialdehyde (MDA) as an index of lipid peroxidation and oxidative stress [64].

Histopathological Examination

Cardiac tissue was fixed in 10% formal saline, dehydrated through ascending grades of ethanol, cleared in xylene,

and embedded in paraffin at 56 °C. Sections of 4–6 µm thickness were mounted, deparaffinised, stained with haematoxylin and eosin, and examined under light microscopy (Olympus BX10) for histoarchitectural changes.

Statistical Analysis

Results are expressed as mean ± SEM (n = 5). Group differences were analysed by one-way analysis of variance (ANOVA) followed by the Newman–Keuls multiple range test using GraphPad InStat version 3.0. A value of $p < 0.05$ was considered statistically significant.

Results

Calibration Curve of Rutin

Absorbance of rutin in ethanol increased proportionally with concentration over the 20–100 µg/mL range, confirming adherence to Beer–Lambert's law and validating the assay for subsequent entrapment-efficiency and drug-release determinations (Table 2, Figure 1).

Table 2. Calibration data for rutin in ethanol.

Concentration (µg/mL)	Absorbance
20	0.162
40	0.261
60	0.431
80	0.587
100	0.686

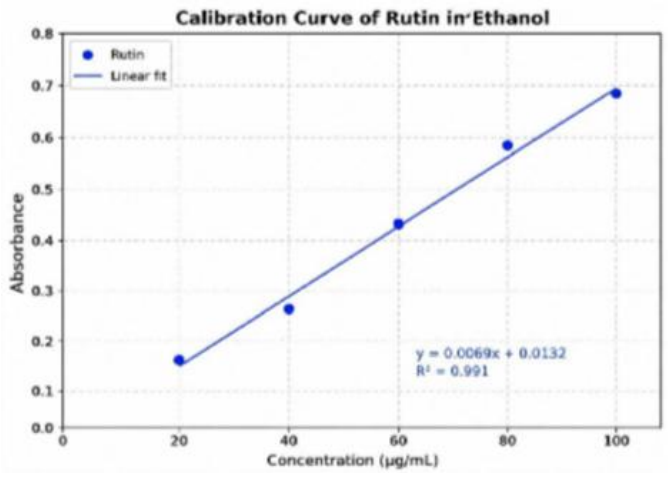

Figure 1. Calibration curve of rutin in ethanol (λmax ≈ 257 nm).

Entrapment Efficiency

The 1:1 rutin-to-phosphatidylcholine formulation (F2) gave the highest entrapment efficiency (94.2%), compared with 88.6% for F1 (1:0.5) and 91.7% for F3 (1:1.5) (Table 3), indicating that an equimolar ratio provided the optimal balance for complex formation. F2 was therefore selected as the optimised formulation for further characterisation and *in vivo* evaluation.

Table 3. Entrapment efficiency of rutin phytosome formulations.

Formulation	Total rutin (mg)	Rutin:PC ratio	Entrapped rutin (mg)	EE (%)
F1	100	1:0.5	88.6	88.6
F2 (optimised)	100	1:1	94.2	94.2
F3	100	1:1.5	91.7	91.7

FTIR Spectroscopy

FTIR spectra of pure rutin and the rutin phytosome retained all major characteristic absorption bands of rutin, with slight shifting and broadening in the O–H (~3430–3400 cm^{-1}), C=O (~1740 cm^{-1}) and C–O (~1270–1240 cm^{-1}) stretching regions of the phytosome spectrum relative to pure rutin (Table 4, Figure 2). These spectral changes are consistent with hydrogen bonding and non-covalent interaction between the polar hydroxyl groups of rutin and the phosphate/glycerol head group of phosphatidylcholine, while the persistence of rutin's aromatic and glycosidic bands confirms that its core chemical structure was preserved after complexation.

Table 4. FTIR band assignments for rutin and rutin phytosome.

Peak (cm^{-1})	Functional group	Rutin	Rutin phytosome	Interpretation
3430–3400	O–H stretch	Present	Present (broadened)	H-bonding at hydroxyl groups
2925–2850	C–H stretch	Weak	More intense	Phospholipid aliphatic chains
1740	C=O stretch	Absent/weak	Present	Phospholipid ester carbonyl
1650–1600	Aromatic C=C	Present	Present	Rutin aromatic ring retained
1270–1240	C–O stretch	Present	Slightly shifted	Rutin–phospholipid interaction
1160–1030	C–O–C/C–O	Present	Present (minor shift)	Glycosidic linkage retained

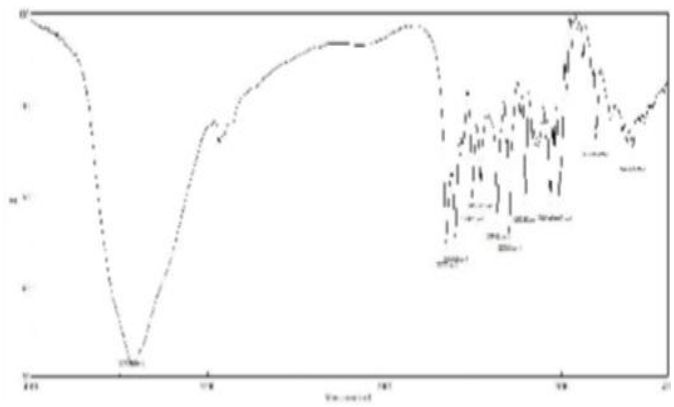

Figure 2a. FTIR spectrum of pure rutin.

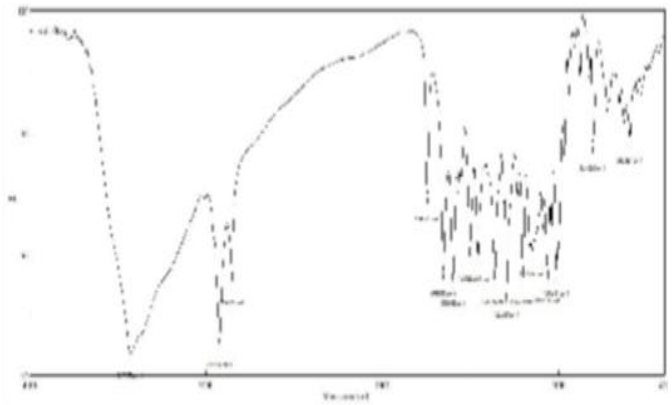

Figure 2b. FTIR spectrum of rutin phytosome.

Scanning Electron Microscopy

SEM of the optimised rutin phytosome revealed irregular, rough-surfaced, predominantly spherical to rounded particles with some aggregation (Figure 3), a morphology typical of phospholipid-based complexes formed by solvent-evaporation techniques and consistent with successful phytosome formation.

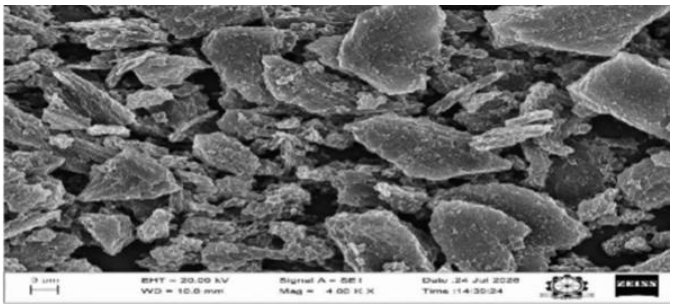

Figure 3. SEM photomicrograph of rutin phytosome (4000×).

In Vitro Drug Release

Rutin phytosome exhibited a gradual, sustained release profile, reaching 83.12% cumulative release at 6 hours (Table 5, Figure 4), rather than a rapid burst release. The initial, relatively faster phase is attributable to diffusion of rutin loosely associated at the vesicle surface, while the slower subsequent phase likely reflects diffusion through the phospholipid matrix.

Table 5. *In vitro* cumulative drug release from rutin phytosome.

Time (h)	Absorbance	Cumulative release (%)
0	0.000	0.00
1	0.169	22.67
2	0.281	38.94
3	0.382	53.71
4	0.472	66.84
5	0.535	75.91
6	0.584	83.12

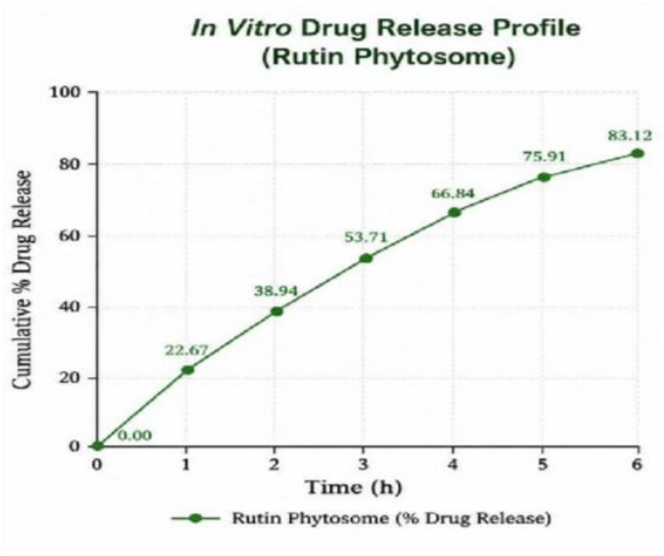

Figure 4. In vitro cumulative drug release profile of rutin phytosome (dialysis membrane method, 6 h).

Cardiac Biomarkers

Doxorubicin administration produced a marked elevation of CK-MB, LDH and troponin-I in the toxic-control group relative to normal control, confirming induction of myocardial injury (Table 6, Figures 5a–c). Pretreatment with carvedilol, rutin, or rutin phytosome significantly reduced all three biomarkers relative to toxic control ($p < 0.001$). The rutin phytosome group showed a greater reduction than the plain-rutin group for all three biomarkers, indicating enhanced cardioprotective activity of the phytosomal formulation.

Table 6. Effect of rutin and rutin phytosome on serum cardiac biomarkers.

Group	CK-MB (U/L)	LDH (IU/L)	Troponin-I (ng/mL)
Normal control	22.50 ± 0.51	180.2 ± 3.19	0.36 ± 0.089
Toxic control	70.40 ± 1.42[a]	471.4 ± 7.16[a]	3.12 ± 0.083[a]
Standard (carvedilol)	31.24 ± 0.58[b]	235.2 ± 4.49[b]	1.06 ± 0.073[b]
Rutin	38.68 ± 0.62[c]	291.4 ± 3.97[c]	2.08 ± 0.020[c]
Rutin phytosome	34.14 ± 0.49[d]	253.2 ± 3.83[d]	0.79 ± 0.037[d]

Values are mean ± SEM (n = 5), analysed by one-way ANOVA followed by the Newman–Keuls multiple range test; $p < 0.001$. [a]vs normal control; [b, c, d]vs toxic control.

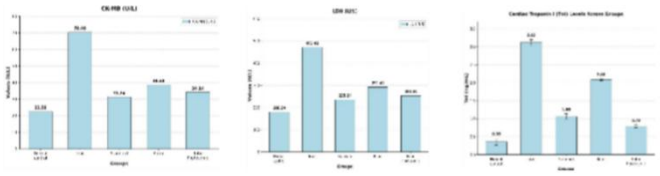

Figure 5. Serum cardiac biomarkers across treatment groups: (a) CK-MB, (b) LDH, (c) Troponin-I.

Myocardial Antioxidant Parameters

Doxorubicin significantly reduced myocardial SOD and CAT activity and increased MDA levels in the toxic-control group relative to normal control, indicating depletion of endogenous antioxidant defences and enhanced lipid peroxidation (Table 7, Figures 6a–c). Treatment with rutin and rutin phytosome improved SOD and CAT activity and reduced MDA relative to toxic control. As reported in the source data set, the standard (carvedilol) group's SOD, CAT and MDA values were numerically closer to those of the toxic control than to the normal control for this parameter set; this is discussed further in Section 4.7 and should be interpreted with appropriate caution pending re-verification against raw instrument data.

Table 7. Effect of rutin and rutin phytosome on myocardial antioxidant parameters.

Group	SOD (U/mg protein)	CAT (µ/min/mg protein)	MDA (µM/mL)
Normal control	20.48 ± 0.24	14.18 ± 0.18	5.48 ± 0.09
Toxic control	9.76 ± 0.21[a]	8.22 ± 0.18[a]	9.72 ± 0.16[a]
Standard (carvedilol)	17.54 ± 0.23[b]	13.56 ± 0.27[b]	5.12 ± 0.09[b]
Rutin	16.02 ± 0.20[c]	12.72 ± 0.17[c]	6.18 ± 0.10[c]
Rutin phytosome	17.45 ± 0.24[d]	13.33 ± 0.25[d]	5.64 ± 0.11[d]

Values are mean ± SEM (n = 5), analysed by one-way ANOVA followed by the Newman–Keuls multiple range test; p < 0.01. [a]vs normal control; [b],[c],[d]vs toxic control.

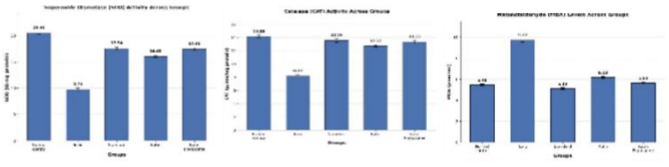

Figure 6. Myocardial antioxidant parameters across treatment groups: (a) SOD, (b) CAT, (c) MDA.

Histopathological Findings

The normal control group showed well-organised myocardial fibres with intact architecture and evenly distributed nuclei, without degenerative or necrotic change (Figure 7a). The toxic-control (doxorubicin-only) group showed disorganised myocardial fibres, widened intercellular spaces and degenerative cellular change, consistent with doxorubicin-induced myocardial injury (Figure 7b). The standard (carvedilol) group showed relatively preserved myocardial fibres with uniform cellular arrangement and intact nuclei, without prominent necrosis (Figure 7c). The rutin-treated group showed moderate cellular activity with spindle-shaped cells arranged in organised bundles and no obvious atypia or necrosis (Figure 7d). The rutin phytosome-treated group showed increased fibroblast proliferation and collagen deposition with reduced inflammatory-cell infiltration, indicating active tissue regeneration (Figure 7e).

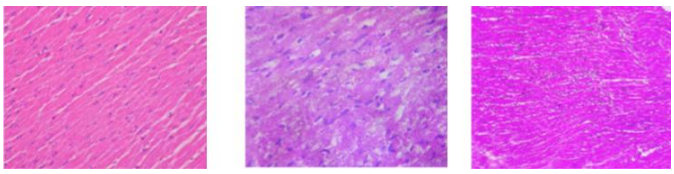

Figure 7. Histopathology (H&E): (a) normal control, (b) toxic control (doxorubicin only), (c) standard (carvedilol).

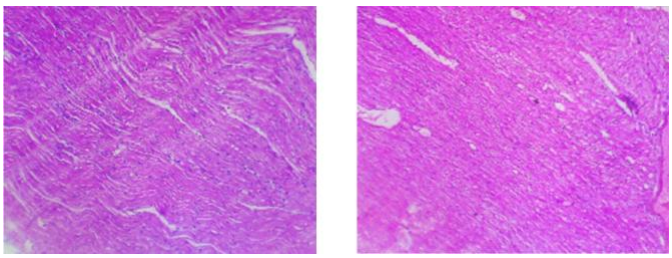

Figure 7 (cont.). (d) Rutin-treated, (e) rutin phytosome-treated.

Discussion

The present study was undertaken to develop a rutin phytosome formulation with improved physicochemical characteristics and to evaluate its cardioprotective potential against doxorubicin-induced cardiotoxicity. Rutin possesses well-documented antioxidant and free-radical-scavenging properties, but its poor aqueous solubility and limited membrane permeability restrict therapeutic utility [16,17]. Complexing rutin with phosphatidylcholine was therefore adopted as a strategy to improve entrapment, stability and controlled release, and thereby bioavailability, for cardioprotective application.

Calibration and Entrapment Efficiency

The linear calibration curve of rutin in ethanol confirmed adherence to Beer–Lambert's law across the tested range, validating its use for entrapment-efficiency and release calculations. Among the three rutin-to-phosphatidylcholine ratios tested, F2 (1:1) gave the highest entrapment efficiency (94.2%), compared with F1 (1:0.5, 88.6%) and F3 (1:1.5, 91.7%). This pattern suggests that an equimolar ratio provides an optimal balance for complexation: at a lower phospholipid ratio, insufficient phosphatidylcholine is available to complex all of the drug, while at a higher ratio, excess uncomplexed phospholipid may compete with the interaction or increase vesicle disorder, marginally lowering entrapment. A comparable dependence of entrapment efficiency on drug-to-phospholipid ratio has been reported for other rutin–phospholipid nanocarriers, in which the molar ratio critically influenced encapsulation

efficiency and colloidal stability [66]. The high entrapment efficiency obtained with F2 supported its selection as the optimised formulation for further evaluation.

FTIR and SEM Characterisation

FTIR comparison of pure rutin and rutin phytosome showed retention of all major characteristic rutin bands, confirming that its core chemical structure remained intact after complexation. The appearance of an ester carbonyl band near 1740 cm^{-1}, together with broadening and slight shifting of the O–H stretching region and increased intensity of aliphatic C–H bands in the phytosome spectrum, indicates non-covalent interaction principally hydrogen bonding between the hydroxyl groups of rutin and the phosphate/glycerol head groups of phosphatidylcholine. This pattern is consistent with earlier reports on rutin–phospholipid complexes, in which new or altered hydroxyl-associated bands were interpreted as direct evidence of molecular complexation rather than simple physical mixing [67]. SEM of the optimised phytosome showed irregular, rough-surfaced, predominantly spherical to rounded particles with some aggregation, a morphology typical of phospholipid complexes formed by solvent-evaporation/hydration techniques in which amphiphilic phosphatidylcholine self-assembles around the drug; the rough, spherical morphology is favourable for effective surface area available for dissolution, corroborating the FTIR evidence of successful complex formation.

In Vitro Drug Release

The optimised rutin phytosome showed a gradual, sustained release profile, reaching approximately 83.1% cumulative release at 6 hours rather than an immediate burst release. The relatively faster initial phase can be attributed to diffusion of rutin loosely associated at or near the vesicle surface, while the slower subsequent phase likely reflects diffusion of the drug through the phospholipid matrix. This biphasic, sustained-release behaviour is characteristic of phospholipid-complexed flavonoids and may prolong systemic exposure to rutin, reduce dosing frequency, and sustain its antioxidant/cardioprotective action relative to a conventional immediate-release formulation.

Cardiac Biomarkers

Doxorubicin administration in the toxic-control group produced a marked increase in CK-MB, LDH and troponin-I relative to normal control, confirming successful induction of cardiotoxicity via myocardial membrane injury. Pretreatment with the standard drug (carvedilol) considerably reduced all three biomarkers. Rutin also reduced these elevated biomarkers, demonstrating a protective effect, and the rutin phytosome group showed a further, greater reduction in CK-MB, LDH and troponin-I than plain rutin. The lower biomarker levels in the phytosome-treated group, relative to the plain-drug group, indicate that phospholipid complexation may have enhanced the cardioprotective activity of rutin, possibly through improved solubility, bioavailability and antioxidant action at the myocardium. Overall, these biomarker findings demonstrate that rutin phytosome provided better protection against doxorubicin-induced myocardial injury than plain rutin, as evidenced by the greater normalisation of all three markers.

Antioxidant Parameters

The toxic-control group showed reduced SOD and CAT activity together with markedly increased MDA, indicating oxidative stress and enhanced lipid peroxidation consequent to doxorubicin-induced cardiotoxicity. Treatment with rutin improved SOD and CAT activity and reduced MDA toward the normal-control value; rutin phytosome produced comparable or numerically greater improvement in SOD, CAT and MDA than plain rutin, consistent with enhanced antioxidant defence and reduced lipid peroxidation. Overall, the antioxidant data indicate that rutin and, to a greater extent, its phytosomal formulation exert protective antioxidant effects against doxorubicin-induced oxidative cardiac injury, restoring SOD and CAT activity and reducing MDA accumulation relative to toxic control.

Histopathological Correlation

The histopathological findings provide morphological support for the biochemical outcomes. The normal-control and standard (carvedilol) groups exhibited well-organised, preserved myocardial fibres with intact architecture and evenly distributed nuclei, establishing a reliable histological baseline. The toxic-control group, which received doxorubicin alone, showed marked fibre disorganisation, widened intercellular spaces and degenerative change pattern consistent with previously reported anthracycline cardiotoxicity models, in which doxorubicin exposure produces myocardial necrosis, cytoplasmic vacuolisation and inflammatory infiltration secondary to oxidative membrane damage. Treatment with rutin and rutin phytosome both produced improvement in myocardial architecture relative to the toxic control. The rutin-treated group showed moderate cellular activity with organised, spindle-shaped cell bundles and no evident atypia or necrosis; the rutin phytosome-treated group showed further improvement, with increased fibroblast proliferation, collagen deposition and reduced inflammatory infiltration, indicating active tissue regeneration. This graded histological recovery — from severe disorganisation in the toxic-control group to more organised, regenerating

architecture in the rutin and, particularly, the rutin phytosome-treated groups — corroborates the proposed antioxidant and anti-apoptotic mechanism of rutin, wherein the flavonoid is thought to attenuate doxorubicin-induced cardiac damage by limiting oxidative membrane injury and excessive apoptosis [69]. The comparatively greater tissue regeneration observed with the phytosomal formulation may reflect improved solubility, membrane permeability and bioavailability conferred by phospholipid encapsulation, enhancing cellular uptake and localised antioxidant activity within the myocardium [70].

Limitations

Several limitations should be considered when interpreting these findings. First, as noted in Section 3.7, the standard (carvedilol) group's antioxidant parameter values (SOD, CAT, MDA) were numerically closer to the toxic-control group than would ordinarily be expected for an established cardioprotectant; these values are reported here exactly as recorded in the study data set, and re-verification against raw instrument/assay records is recommended before the antioxidant findings for the standard group are relied upon in isolation. This inconsistency does not affect the cardiac-biomarker or histopathological findings, which showed the expected direction and magnitude of protective effect for all treatment groups relative to toxic control. Second, the study evaluated a single dose level of rutin and rutin phytosome (50 mg/kg) and a single time point (Day 16); dose–response and pharmacokinetic studies, including plasma and myocardial tissue concentration profiling of rutin versus rutin phytosome, would strengthen mechanistic and translational conclusions. Third, histopathological assessment was qualitative/descriptive rather than based on a validated semi-quantitative injury scoring system, and did not include specific stains for fibrosis (e.g., Masson's trichrome) or markers of apoptosis (e.g., TUNEL, caspase-3 immunohistochemistry), which would allow more precise mechanistic correlation with the proposed antioxidant and anti-apoptotic pathway. Finally, the effect of rutin phytosome on doxorubicin's antitumour efficacy was not assessed in this model and would need to be established in a tumour-bearing model before any adjuvant clinical application could be considered.

Conclusion

This study successfully developed and characterised a rutin phytosome formulation to overcome the poor aqueous solubility and limited membrane permeability of plain rutin. The optimised formulation (F2, 1:1 rutin-to-phosphatidylcholine ratio) showed the highest entrapment efficiency (94.2%), and FTIR and SEM analyses confirmed stable complex formation with preservation of rutin's core structure. The formulation exhibited sustained *in vitro* release of approximately 83.1% over 6 hours, favouring prolonged systemic exposure.

In the *in vivo* model, doxorubicin produced significant cardiac injury, reflected in elevated CK-MB, LDH and troponin-I, reduced SOD and CAT activity, and increased MDA levels. Pretreatment with rutin phytosome attenuated these changes more effectively than free rutin, indicating that phospholipid complexation improved rutin's cardioprotective efficacy, most plausibly through enhanced bioavailability and antioxidant action at the myocardium. This biochemical protection was corroborated histopathologically by a graded restoration of myocardial architecture, from severe disorganisation in the doxorubicin-only group to a more organised, regenerating structure in the phytosome-treated group.

Overall, phytosomal complexation appears to be an effective strategy for enhancing the physicochemical and biopharmaceutical properties of rutin, conferring greater protection against doxorubicin-induced cardiotoxicity than native rutin, most likely through combined antioxidant, anti-inflammatory and anti-apoptotic mechanisms. Rutin phytosome may therefore hold promise as an adjuvant cardioprotective agent alongside doxorubicin-based chemotherapy, warranting further dose–response, pharmacokinetic and tumour-bearing-model studies, together with re-verification of the standard-group antioxidant data noted in Section 4.7, to establish clinical applicability.

Acknowledgement

The authors thank the Department of Pharmacology, K.M. College of Pharmacy, Madurai, for providing the facilities used in this study.

References

1. Bray F, Laversanne M, Sung H, Ferlay J, Siegel RL, Soerjomataram I, Jemal A. Global cancer statistics 2022: GLOBOCAN estimates of incidence and mortality worldwide for 36 cancers in 185 countries. CA Cancer J Clin. 2024;74(3):229-263.
2. International Agency for Research on Cancer (IARC). GLOBOCAN 2022: Latest global cancer data shows rising incidence and stark inequities. Union for International Cancer Control; 2024.
3. Wang S, Kotamraju S, Konorev E, Kalivendi S, Joseph J, Kalyanaraman B. Activation of nuclear factor-kappaB during doxorubicin-induced apoptosis in endothelial cells and myocytes is pro-apoptotic: the role of hydrogen peroxide. Biochem J. 2002;367(Pt 3):729-740.
4. Songbo M, Lang H, Xinyong C, Bin X, Ping Z, Liang S. Oxidative stress injury in doxorubicin-induced cardiotoxicity. Toxicol Lett. 2019;307:41-48.
5. Wallace KB, Sardão VA, Oliveira PJ. Mitochondrial determinants of doxorubicin-induced cardiomyopathy. Circ Res. 2020;126(7):926-941.

6. Al Khafaji M, et al. Managing doxorubicin cardiotoxicity: insights into molecular mechanisms and protective strategies. J Biochem Mol Toxicol. 2025;39(2):e70155.
7. Zhang S, Liu X, Bawa-Khalfe T, Lu LS, Lyu YL, Liu LF, Yeh ET. Identification of the molecular basis of doxorubicin-induced cardiotoxicity. Nat Med. 2012;18(11):1639-1642.
8. Christidi E, Brunham LR. Regulated cell death pathways in doxorubicin-induced cardiotoxicity. Cell Death Dis. 2021;12(4):339.
9. Belger C, et al. A review of the pathophysiological mechanisms of doxorubicin-induced cardiotoxicity and aging. NPJ Aging. 2024;10(1):1.
10. Cardio-oncology's modern approaches to prevent doxorubicin-induced cardiotoxicity: a systematic review. 2024.
11. Al-Kuraishy HM, Al-Gareeb AI, et al. Cardioprotective strategies against doxorubicin-induced cardiotoxicity: a review from standard therapies to emerging mitochondrial transplantation. Biomed Pharmacother. 2025.
12. Reichardt P, Tabone MD, Mora J, Morland B, Jones RL. Dexrazoxane in cardioprotection during anthracycline therapy: a systematic review. IntechOpen. 2024.
13. Geest V, et al. Dexrazoxane protects against doxorubicin-induced cardiotoxicity in susceptible human living myocardial slices: a proof-of-concept study. Br J Pharmacol. 2025.
14. Lyu Y, Wagner JR, et al. Dexrazoxane to prevent cardiotoxicity in adults treated with anthracyclines: JACC CardioOncology controversies. J Am Coll Cardiol CardioOnc. 2024;6(2):322-324.
15. Syahputra RA, Harahap U, Dalimunthe A, Nasution MP, Satria D. The role of flavonoids as a cardioprotective strategy against doxorubicin-induced cardiotoxicity: a review. Molecules. 2022;27(4):1320.
16. Ganeshpurkar A, Saluja AK. The pharmacological potential of rutin. Saudi Pharm J. 2017;25(2):149-164.
17. Chua LS. A review on plant-based rutin extraction methods and its pharmacological activities. J Ethnopharmacol. 2013;150(3):805-817.
18. Al-Rejaie SS, et al. Cardioprotective effects of rutin via alteration in TNF-α, CRP, and BNP levels coupled with antioxidant effect in STZ-induced diabetic rats. Mol Cell Biochem. 2016.
19. 19. Singh D, Rawat M, Semalty A, Semalty M. Rutin-phospholipid complex: an innovative technique in novel drug delivery system (NDDS). Curr Drug Deliv. 2012;9(3):305-314.
20. Barani M, Sangiovanni E, Angarano M, et al. Phytosomes as innovative delivery systems for phytochemicals: a comprehensive review of literature. Int J Nanomedicine. 2021;16:6983-7022.
21. Weiss RB. The anthracyclines: will we ever find a better doxorubicin? Semin Oncol. 1992;19(6):670-686.
22. DOXOrubicin Monograph for Professionals. Drugs.com; 2026.
23. Tacar O, Sriamornsak P, Dass CR. Doxorubicin: an update on anticancer molecular action, toxicity and novel drug delivery systems. J Pharm Pharmacol. 2013;65(2):157-170.
24. Thorn CF, Oshiro C, Marsh S, et al. Doxorubicin pathways: pharmacodynamics and adverse effects. Pharmacogenet Genomics. 2011;21(7):440-446.
25. Christoforidou A, et al. Physiologically based pharmacokinetic modelling and simulation to predict the plasma concentration profile of doxorubicin. Pharmaceutics. 2022;14(9):1892.
26. Songbo M, Lang H, Xinyong C, Bin X, Ping Z, Liang S. Oxidative stress injury in doxorubicin-induced cardiotoxicity. Toxicol Lett. 2019;307:41-48.
27. Zhang S, Liu X, Bawa-Khalfe T, et al. Identification of the molecular basis of doxorubicin-induced cardiotoxicity. Nat Med. 2012;18(11):1639-1642.
28. Wallace KB, Sardão VA, Oliveira PJ. Mitochondrial determinants of doxorubicin-induced cardiomyopathy. Circ Res. 2020;126(7):926-941.
29. National Center for Biotechnology Information. PubChem Compound Summary for CID 31703, Doxorubicin. PubChem; 2026.
30. Farzam K, Jan A. Beta blockers. In: StatPearls. Treasure Island, FL: StatPearls Publishing; 2023.
31. McTavish D, Campoli-Richards D, Sorkin EM. Carvedilol: a review of its pharmacodynamic and pharmacokinetic properties, and therapeutic efficacy. Drugs. 1993;45(2):232-258.
32. Feuestein GZ, Ruffolo RR Jr. Pharmacology of carvedilol. Am J Cardiol. 2004;93(9A):3B-6B.
33. Yue TL, Cheng HY, Lysko PG, et al. Carvedilol, a new vasodilator and beta adrenoceptor antagonist, is an antioxidant and free radical scavenger. J Pharmacol Exp Ther. 1992;263(1):92-98.
34. DrugBank. Carvedilol: Uses, Interactions, Mechanism of Action. DrugBank Online; 2026.
35. Yu X, Cui L, Zhang Z, Zhao Q, Li S. Carvedilol attenuates inflammatory-mediated cardiotoxicity in daunorubicin-induced rats. Pharmacology. 2013;92(1-2):18-27.
36. GoodRx Health. Carvedilol mechanism of action: how does carvedilol work? GoodRx; 2023.
37. Ganeshpurkar A, Saluja AK. The pharmacological potential of rutin. Saudi Pharm J. 2017;25(2):149-164.
38. 38. Chua LS. A review on plant-based rutin extraction methods and its pharmacological activities. J Ethnopharmacol. 2013;150(3):805-817.
39. Sharma S, Ali A, Ali J, Sahni JK, Baboota S. Rutin: therapeutic potential and recent advances in drug delivery. Expert Opin Investig Drugs. 2013;22(8):1063-1079.
40. .A review on the chemistry and biological properties of rutin. Asian J Pharm Pharmacol. 2019;5(S1):1-20.
41. Manach C, Morand C, Demigné C, Texier O, Régérat F, Rémésy C. Bioavailability of rutin and quercetin in rats. FEBS Lett. 1997;409(1):12-16.
42. Rutin - an overview. ScienceDirect Topics; 2026.
43. Chen T, Li LP, Lu XY, Chen HR, Zhu YM, Zhou HY. Absorption and metabolism characteristics of rutin in Caco-2 cells. ScientificWorldJournal. 2013;2013:382350.
44. National Center for Biotechnology Information. PubChem Compound Summary for CID 5280805, Rutin. PubChem; 2026.
45. Patel K, Patel DK. Rutin - an overview. In: Bioactive Food as Dietary Interventions for Arthritis and Related Inflammatory Diseases. 2nd ed. Academic Press; 2019.
46. Rahmani AH, Alsahli MA, Almatroudi A, et al. The protective effects of rutin on the liver, kidneys, and heart by counteracting organ toxicity caused by synthetic and natural compounds. Food Sci Nutr. 2023;11(2):675-687.
47. Singh D, Rawat M, Semalty A, Semalty M. Rutin-phospholipid complex: an innovative technique in novel drug delivery system (NDDS). Curr Drug Deliv. 2012;9(3):305-314.
48. Barani M, Sangiovanni E, Angarano M, et al. Phytosomes as innovative delivery systems for phytochemicals: a comprehensive review of literature. Int J Nanomedicine. 2021;16:6983-7022.
49. Van Hoogevest P, Wendel A. The use of natural phospholipids as pharmaceutical excipients. Pharma Excipients; 2020.
50. Lecithin - an overview. ScienceDirect Topics; 2026.
51. Cosmetic Ingredient Review. Safety assessment of lecithin and other phosphoglycerides as used in cosmetics. CIR; 2015.
52. Wang H, Cui Y, Fu Q, et al. A phospholipid complex to improve the oral bioavailability of flavonoids. Drug Dev Ind Pharm. 2015;41(10):1693-1703.
53. Kalmegh N, Laware S. Rutin phytosome for diabetes: formulation and evaluation. Int J Pharm Sci Res. 2016.
54. Sharma S, Parashar M, Lal K, Naik M, Tanwar SS. Doxorubicin-induced cardiotoxicity: comprehensive pathway insights and advanced preclinical therapeutics. 2026.

55. Sun ML, Dong JM, Liu C, Li P, Zhang C, Zhen J, Chen W. Metformin-mediated protection against doxorubicin-induced cardiotoxicity. 2024.
56. Karakuyu NF, et al. Investigation of cardioprotective effect of lercanidipine on doxorubicin-induced cardiotoxicity. 2023.
57. AlQahtani AA, et al. Cardioprotective effect of marine astaxanthin on doxorubicin-induced cardiotoxicity in normal rats. [Journal details as available in original article].
58. Wang YD, Zhang Y, Sun B, Leng XW, Li YJ, Ren LQ. The cardioprotective effects of rutin against pirarubicin-induced cardiotoxicity in rats. 2018.
59. Vu HT, Hook SM, Siqueira SD, Müllertz A, Rades T, McDowell A. Phytosomes as a nanodelivery system for the antioxidant rutin. 2018.
60. Ganeshpurkar A, Saluja AK. The pharmacological potential of rutin. Saudi Pharmaceutical Journal. 2017.
61. Vankudri R, Habbu P, Hiremath M, Patil BS, Savant C. Development and evaluation of a rutin-phospholipid complex for therapeutic efficacy and bioavailability of rutin. 2016.
62. Varshney P, et al. Cardioprotective effect of Solanum nigrum against doxorubicin-induced cardiotoxicity. [Journal details as available in original article].
63. Formulation of Phytosomes with Extracts of Ginger Rhizomes and Rosehips with Improved Bioavailability, Antioxidant and Anti-Inflammatory Effects *In Vivo*.2025.
64. Viswanatha Swamy AHM, Wangikar U, Koti BC, Thippeswamy AHM, Ronad PM, Manjula DV. Cardioprotective effect of ascorbic acid on doxorubicin-induced myocardial toxicity in rats. Indian J Pharmacol. 2011
65. Gupta S.K. et al., Effect of rutin on retinal VEGF, TNF-α, aldose reductase and total antioxidant capacity in diabetic rats. International Ophthalmology, 2019.
66. Babazadeh A, Ghanbarzadeh B, Hamishehkar H. Phosphatidylcholine-rutin complex as a potential nanocarrier for food applications. J Funct Foods. 2017;33:134–141.
67. Vu HTH, Hook SM, Siqueira SD, Müllertz A, Rades T, McDowell A. Are phytosomes a superior nanodelivery system for the antioxidant rutin? Int J Pharm. 2018;548(1):82–91.
68. Mahmoud HUR, Ahmed OM, Fahim HI, Ahmed NA, Ashour MB. Effects of rutin and quercetin on doxorubicin-induced renocardiotoxicity in male Wistar rats. Adv Anim Vet Sci. 2020;8(4):e1-e13.
69. Ma Y, Yang L, Ma J, Lu L, Wang X, Ren J, Yang J. Rutin attenuates doxorubicin-induced cardiotoxicity via regulating autophagy and apoptosis. Biochim Biophys Acta Mol Basis Dis. 2017;1863(8):1904–1911.
70. Salama, A.F., Kasem, S.M., Abdel Rahman, M.A. and Abdel-Wahhab, K.G. (2020). Effects of Rutin and Quercetin on Doxorubicin-Induced Renocardiotoxicity in Male Wistar Rats. Advances in Animal and Veterinary Sciences, 8(4), 370–384. https://doi.org/10.17582/journal.aavs/2020/8.4.370.384.